Influence of Crowding on Hydrophobic Hydration-Shell Structure

Aria J. Bredt and Dor Ben-Amotz

Purdue University, Department of Chemistry, West Lafayette, IN 47907

SUPPLEMENTARY INFORMATION

The following supplementary materials are provided in this document:

1) A description of the Muller-like model as applied to hydration-shell crossover behavior.
2) Implications regarding Hydration-shell spectral shape.
3) Crossover temperature correlation results for alcohol solutes.
4) Additional Raman-MCR results for TBA, 2BA, and BE.
5) Additional plots for the three solutes (similar to Fig. 4 in the parent manuscript).
6) MD predictions for the hydration-shell coordination numbers of the three solutes vs. T and [c].

1) Muller-Like Model of Water Structure. In the spirit of the Muller model,[1] we may describe the structure of water in terms of an equilibrium between structures with (*H*) and (*L*) disorder. In other words, roughly speaking, these two structures correspond to liquid-like (*H*) and clathrate-like or ice-like (*L*) structures (and the former structure is favored at high temperature while the latter is favored at low temperature). The equilibrium between these two structures, $H \rightleftharpoons L$, may be described thermodynamically, as follows.

$$K = \frac{[L]}{[H]} \tag{S1}$$

$$\Delta G = -RT \ln K = \Delta H - T\Delta S \tag{S2}$$

$$\Delta H = \left[\frac{\partial(\Delta G/T)}{\partial(1/T)}\right]_P = RT^2 \left(\frac{\partial \ln K}{\partial T}\right)_P \tag{S3}$$

$$\Delta S = -\left(\frac{\partial \Delta G}{\partial T}\right)_P = \frac{\Delta H - \Delta G}{T} \tag{S4}$$

Note that ΔG and the other thermodynamic state function changes are equivalent to the difference between the corresponding Ben-Naim solvation thermodynamic functions[2] for water in the *L* and *H* structures. Since the population of the more ordered structure decreases with increasing temperature, the temperature derivative of $\ln K$ is negative, and thus $\Delta H < 0$ and $\Delta S < 0$. Note that the latter inequality follows from the fact that the transformation is expressed as that from the more disordered to the more ordered structure. The signs of ΔH and ΔS necessarily hold both in bulk water and in the hydration-shell of an oily solute, but the values of the corresponding enthalpy and entropy changes need not be the same in the bulk (ΔH_B and ΔS_B) as they are in the hydration-shell (ΔH_S and ΔS_S). Moreover, the occurrence of a crossover temperature implies that the temperature derivative of $\ln K$ in the hydration-shell has a larger magnitude than that in the bulk, and thus $\Delta H_S < \Delta H_B < 0$. Furthermore, at the crossover temperature $\Delta G_S(T^*) = \Delta G_B(T^*)$, because at that temperature the equilibrium constant, *K,* is the same in both regions, and thus $\Delta H_S - T^* \Delta S_S = \Delta H_B - T^* \Delta S_B$, which implies that the crossover temperature may be expressed as follows.

$$T^* = \frac{\Delta H_S - \Delta H_B}{\Delta S_S - \Delta S_B} \tag{S5}$$

Note that since T^* is positive and $\Delta H_S - \Delta H_B$ is negative, that necessarily implies that $\Delta S_S - \Delta S_B$ must also be negative. In other words, the existence of a hydration-shell crossover temperature implies that both the enthalpy and entropy differences between the ordered and disordered water structures are larger (more negative) in the hydration-shell than in bulk water. If it is further assumed that $\Delta S_S - \Delta S_B$ is less sensitive to solutes size and crowding than $\Delta H_S - \Delta H_B$, that would imply that a solute with a larger T^* is one for which the ordered hydration-shell structure is more enthalpically stabilized (has a more negative ΔH_S) than it is for a solute that has a smaller T^*. In other words, this implies that a solute with a higher T^* is one whose shape is such that it can better stabilize a clathrate-like water structure.

The above assumption regarding the relationship between $\Delta S_S - \Delta S_B$ and $\Delta H_S - \Delta H_B$ is consistent with the expectation that the entropy difference between ordered and disordered water structures is dictated primarily by the tetrahedrality of water, rather than by its interaction with the solute, while the enthalpy difference between the ordered and disordered water structures is expected to be strongly influenced by solute-water interactions and thus to be sensitive to solute size, shape, and crowding.

2) Implications Regarding Hydration-Shell Spectral Shape. Our identification of the crossover temperature as the temperature at which $\Delta\omega$ changes sign relies on the following implicit assumptions and mathematical implications. In order for $\Delta\omega$ to change sign the SC OH band spectrum must have a mean frequency that itself crosses from a lower to a higher frequency than the OH band of pure water as a function of temperature. More specifically, the SC and pure water spectra must be obtained at the same temperatures, the same integration bounds must be used to obtain the average OH frequency. Thus, the observation of $\Delta\omega$ crossover implies that SC spectrum must have a shape that is temperature dependent, and thus may be viewed as consisting of sub-bands of different temperature dependence. These general criteria are satisfied by the SC spectra of the three solutes in Figure 1, as well as by the solutes whose hydration-shell spectra have previously been found to undergo a crossover.[3-6] Moreover, our observation that the SC hydration-shell OH stretch bands have a temperature dependent shape is also qualitatively consistent with THz observations that the low frequency hydration-shell spectra of aqueous alcohol solutions consist of sub-bands of different temperature dependence.[7]

It is also important to note that a crossover in $\Delta\omega$ need not in general imply that the corresponding hydration-shell spectrum (and thus the hydration-shell structure) is similar to that of bulk water. For example, if a SC spectrum consisted of two bands (of arbitrarily large intensity) whose mean frequency was the same as the pure water OH band then the value of $\Delta\omega$ would necessarily be zero but the spectral shape of the hydration-shell might be quite different from that of pure water. Thus, a crossover in the sign of $\Delta\omega$ only implies that the hydration-shell spectrum is similar to water if the intensity of the SC spectrum is also minimized near the crossover temperature, as is the case with all of the SC hydration-shell spectra

of interest in this work. In other words, as previously shown[6] the crossover temperature obtained from the temperature at which $\Delta\omega$ crosses zero is also invariably near the temperature at which the SC spectrum has a minimum area. Note that the fact that the SC spectra have an area that is minimized near the crossover temperature is also evident in the spectra shown in Figure 3A and 3B of the parent manuscript, as well as Figures S1-S3 below.

Finally, note about the invariance of the crossover temperature to the assumed size of the hydration-shell is consistent with fact that SMCR decomposes the measured spectrum into a linear combination of the pure water and SC spectra. Thus, the temperature at which $\Delta\omega$=0 is that at which the mean frequency of the SC spectrum is equal to the mean frequency of the corresponding pure water spectrum. This also implies that at the crossover temperature any linear combination of the two pure water and SC spectra must also have the same mean frequency as pure water. Since the assumed number of water molecules in the hydration-shell only changes the relative weights of the pure water and SC spectrum in the total hydration-shell spectrum, the crossover temperature must be independent of the assumed hydration-shell size.

3) Crossover Temperature Correlation. The following table contains crossover temperatures at infinite dilution for 6 alcohol solutes, as well as the solvent accessible surfaces area (SASA) and number of methyl groups (nCH_3) of each solute. The fit values T_0^* in the last column are predicted using the following expression (fit to the experimental data points): T_0^*(°C) = 314.9 -1.026*SASA + 6.36*nCH_3.

Table S1. Crossover temperature correlation for alcohol solutes.

Solute	SASA (Å^2)	nCH$_3$	T_0^* (Expt.) (°C)	T_0^* (Fit) (°C)
Methanol	155.6	1	164	162
Ethanol	191.8	1	120	125
1-Propanol	222.3	1	95	93
1-Butanol	252.7	1	62	62.
2BA	246.1	2	76.5	75.2
TBA	240.5	3	86.7	87.2

4) Additional Raman-MCR Results. The following three figures contain temperature and concentration dependent SC spectra of TBA, 2BA, and BE.

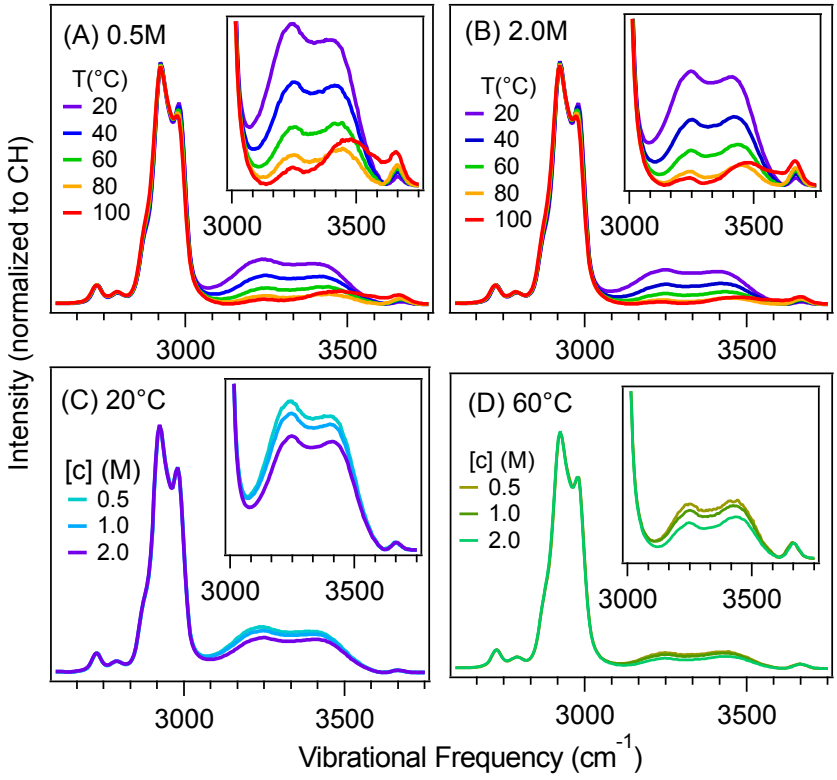

Figure S1. The influence of temperature and concentration on the Raman-MCR SC spectra of aqueous tert-butyl alcohol (TBA), in the solute CH and hydration-shell OH band regions. (A) and (B) compare the temperature dependence of the SC spectra at solute concentrations of 0.5M and 2M. (C) and (D) compare the concentration dependence of the SC spectra at 20°C and 60°C. All the spectra are normalized to the

CH band area, and thus represent the average SC spectra of a single solute. The inset panel contain an expanded view of the SC hydration-shell (OH band) spectra, all plotted on the same scale.

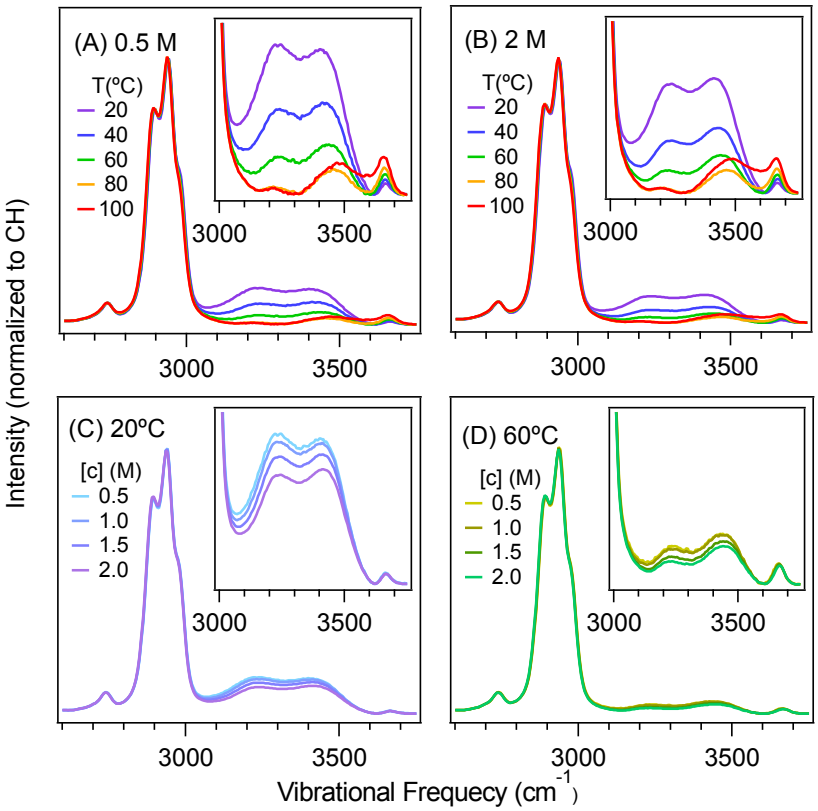

Figure S2. The influence of temperature and concentration on the Raman-MCR SC spectra of aqueous 2-Butanol, in the solute CH and hydration-shell OH band regions. (A) and (B) compare the temperature dependence of the SC spectra at solute concentrations of 0.5M and 2M. (C) and (D) compare the concentration dependence of the SC spectra at 20°C and 60°C. All the spectra are normalized to the CH band area, and thus represent the average SC spectra of a single solute. The inset panel contain an expanded view of the SC hydration-shell (OH band) spectra, all plotted on the same scale.

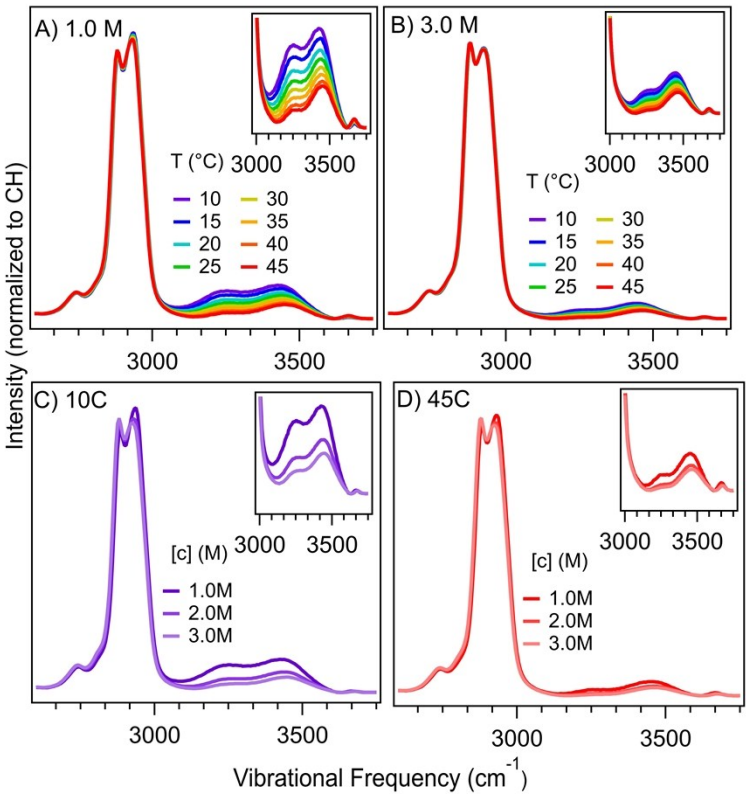

Figure S3. The influence of temperature and concentration on the Raman-MCR SC spectra of aqueous 2-butoxyethanol (BE), in the solute CH and hydration-shell OH band regions. (A) and (B) compare the temperature dependence of the SC spectra at solute concentrations of 1M and 3M. (C) and (D) compare the concentration dependence of the SC spectra at 10°C and 45°C. All the spectra are normalized to the CH band area, and thus represent the average SC spectra of a single solute. The inset panel contain an expanded view of the SC hydration-shell (OH band) spectra, all plotted on the same scale.

5) Additional Crossover Results. The following three figures are similar to Fig. 4 in the parent manuscript, except for the addition of the dot-dashed curves obtained assuming that the first hydration-shell coordination number is equal to its predicted value at infinite dilution (ID). The solid curves in Fig. 4 and the following three figures are obtained assuming that the first hydration-shell coordination numbers decrease with increasing solute concentration, as predicted using the MD simulations (see Figs. S7 and S8, and Table S2). The dashed curves in Fig. 4 and the following three figures assume that all the water molecules in the solution are in the hydration-shell of the solute. The agreement between the crossover temperatures obtained using these three assumptions confirms that the experimentally derived crossover temperatures are insensitive to the assumed hydration-shell coordination numbers.

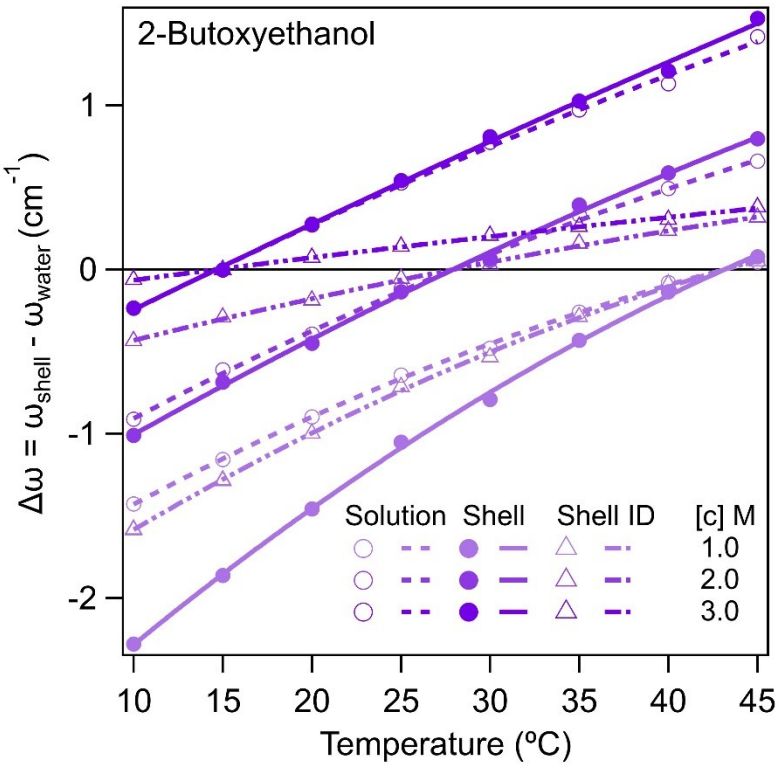

Figure S4. Hydration-shell structural crossover is quantified by comparing the average OH frequency in the hydration-shell with that in bulk water as a function of solute concentration. The crossover may be obtained either from the OH bands of the measured solution and water spectra (open circular point and dashed lines) or from the OH bands of the Raman-MCR reconstructed first hydration-shells (solid points and lines) or from the OH bands of the first hydration-shells at infinite dilution (ID, open triangular point and dashed lines). All procedures yield similar crossover temperatures that decrease with increasing solute concentration.

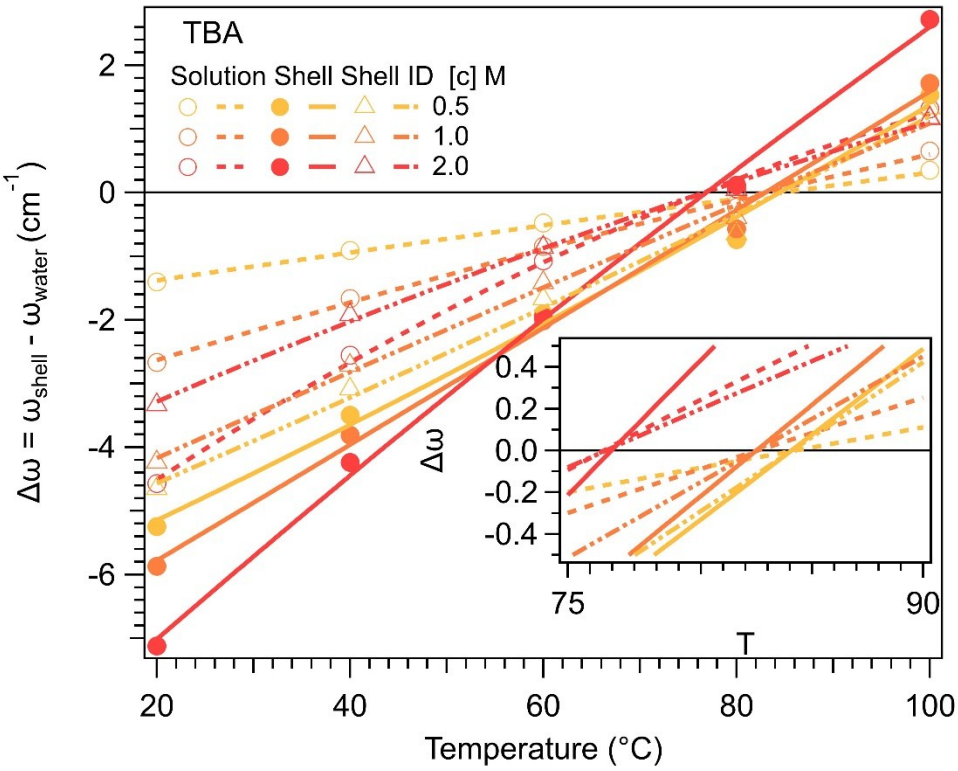

Figure S5. Hydration-shell structural crossover is quantified by comparing the average OH frequency in the hydration-shell with that in bulk water as a function of solute concentration. The crossover may be obtained either from the OH bands of the measure solution and water spectra (open circular points and dashed lines) or from the OH bands of the Raman-MCR reconstructed first hydration-shells (solid circular points and lines) or from the OH bands of the first hydration-shells at infinite dilution (ID, open triangular point and dashed lines). All procedures yield similar crossover temperatures that decrease with increasing solute concentration.

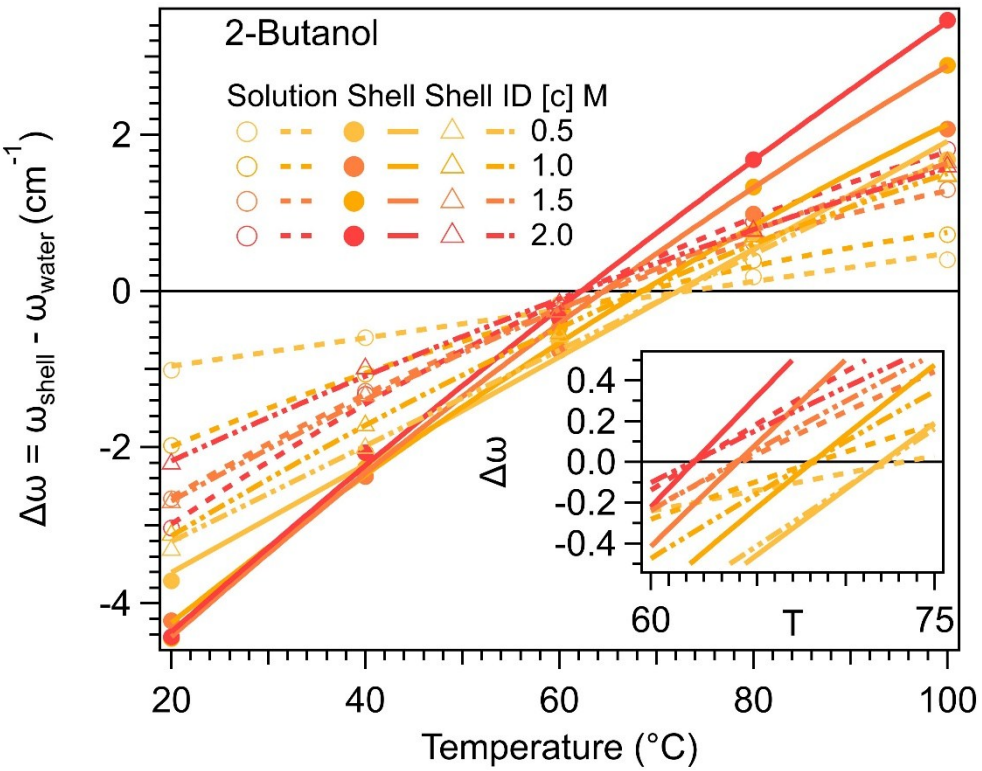

Figure S6. Hydration-shell structural crossover is quantified by comparing the average OH frequency in the hydration-shell with that in bulk water as a function of solute concentration. The crossover may be obtained either from the OH bands of the measure solution and water spectra (open circular points and dashed lines) or from the OH bands of the Raman-MCR reconstructed first hydration-shells (solid circular points and lines) or from the OH bands of the first hydration-shells at infinite dilution (ID, open triangular point and dashed lines). All procedures yield similar crossover temperatures that decrease with increasing solute concentration.

6) MD Coordination Numbers Predictions. The MD coordination number simulations were performed using GROMACS[8] as previously described,[6] with the following additional details. The solute and water potentials are TraPPE-UA[9] and TIP4P/2005,[10] respectively. The simulations were each run for 100 ns (after 5 ns of pre-equilibration) with 256 water molecules and a variable number of solute molecules, spanning a concentration range between 0.2 M and 4 M. Given the relatively small system size of these simulations (with 256 water molecules), one does not expect the simulations to accurately describe solute aggregation statistics, and particularly the formation of higher-order solute clusters. However, this limitation does not influence our conclusions, as the simulations results are used only to obtain estimates of the hydration-shell

coordination numbers, and to show that the resulting experimentally-derived crossover temperatures are insensitive to the assumed coordination number values.

Figure S7 shows representative examples of the radial distribution function for the water oxygen around any solute carbon atom. The water coordination numbers were obtained by integrating the total number of unique water molecules out to a cut-off distance of 0.636 nm from any solute carbon atom (as indicated by the dashed vertical line in Fig. S7). The term unique indicates that water molecules that are within the cut-off distance from more than one solute carbon atom are only counted once.

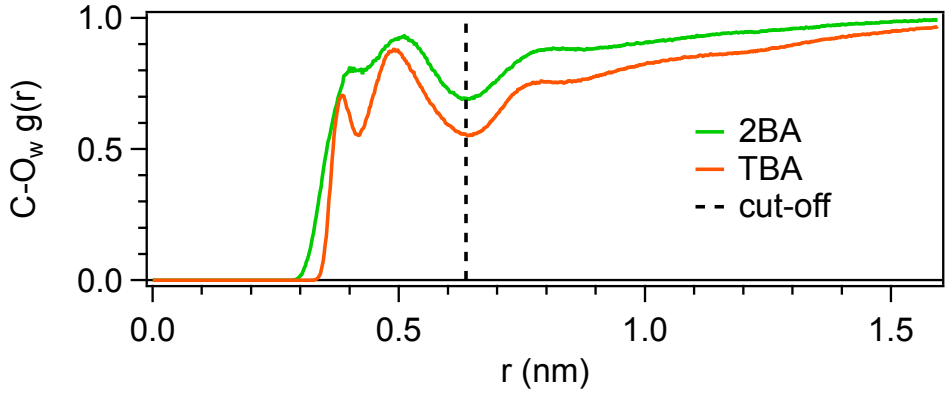

Figure S7. Radial distribution functions between solute carbon and water oxygen atoms of 2BA and TBA obtained at 323.15K (50ºC). The vertical dashed line indicates the cut-off value of 0.636 nm that is used to obtain the water coordination numbers surrounding the carbon atoms of all three solutes.

Figure S8 shows MD predictions of the hydration-shell coordination numbers for the three solutes as a function of temperature and concentration, obtained as previously described.[6] Table S2 contains the polynomial fit coefficients that can be used to re-generate the coordination number predictions. The temperature dependent coefficients, K0-K3 are those used to obtain the coordination numbers (CN) using the bottom equations in Table S2. The temperature (T) is in Kelvin units (equal to T ºC+273.15), and the solute concentration (conc) is in M units.

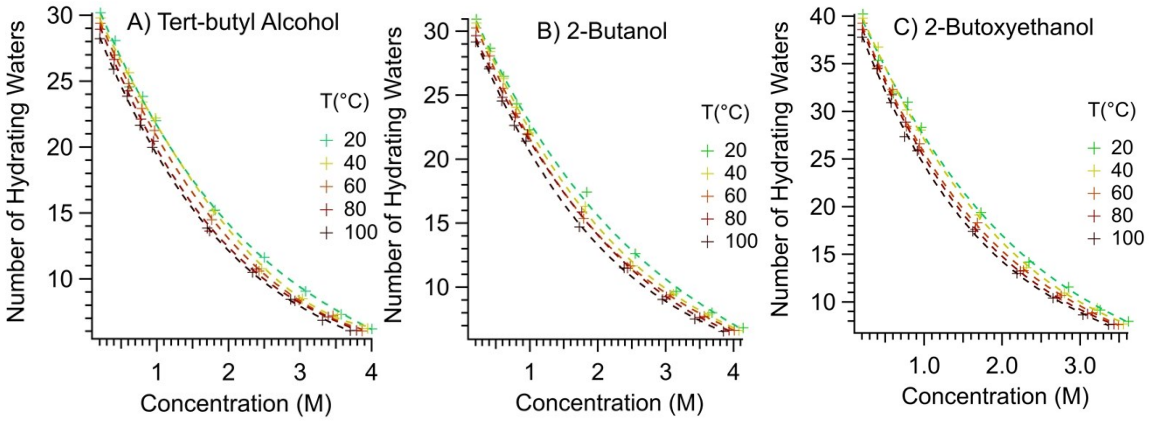

Figure S8. The calculated number of waters in the first hydration shell of the solute CH_2 or CH_3 groups obtained from MD simulations of (A) tert-butyl alcohol (TBA), (B) 2-butanol (2BA) and (C) 2-butoxyethanol (BE), as a function of temperature and concentration.

Table S2. Polynomial fit to the MD coordination numbers.

A) Tert-butyl Alcohol	B) 2-Butanol	C) 2-Butoxyethanol
$K0=21.325+0.084938*(T)-0.00015666*(T^2)$	$K0=13.461+0.13864*(T)-0.00024012*(T^2)$	$K0=0.10603+0.28822*(T)-0.00047158*(T^2)$
$K1=-16.619+0.040578*(T)-9.3318E-05*(T^2)$	$K1=40.849-0.31209*(T)+0.00044729*(T^2)$	$K1=82.505-0.60592*(T)+0.00087212*(T^2)$
$K2=16.991-0.10182*(T)+0.00017186*(T^2)$	$K2=-15.16+0.0981570*(T)-0.00013698*(T^2)$	$K2=-42.205-0.26817*(T)-0.00037894*(T^2)$
$K3=-3.4604+0.021814*(T)-3.5254E-05*(T^2)$	$K3=1.2094-0.075331*(T)+1.033-05*(T^2)$	$K3=5.7889+0.035231*(T)-4.9524-05*(T^2)$
resulting coordination number equation	resulting coordination number equation	resulting coordination number equation
$CN=K0+K1*(conc)+K2*(conc^2)+K3*(conc^3)$	$CN=K0+K1*(conc)+K2*(conc^2)+K3*(conc^3)$	$CN=K0+K1*(conc)+K2*(conc^2)+K3*(conc^3)$

References

1. N. Muller, Search for a Realistic View of the Hydrophobic Effect, *Acc. Chem. Res.*, 1990, **23**, 23-28.
2. A. Ben-Naim, *Solvation thermodynamics*, Plenum Press, New York, 1987.
3. J. G. Davis, K. P. Gierszal, P. Wang and D. Ben-Amotz, Water structural transformation at molecular hydrophobic interfaces, *Nature*, 2012, **491**, 582-585.
4. J. G. Davis, S. R. Zukowski, B. M. Rankin and D. Ben-Amotz, Influence of a Neighboring Charged Group on Hydrophobic Hydration Shell Structure, *J. Phys. Chem. B*, 2015, **119**, 9417−9422.
5. X. E. Wu, W. J. Lu, L. M. Streacker, H. S. Ashbaugh and D. Ben-Amotz, Temperature-Dependent Hydrophobic Crossover Length Scale and Water Tetrahedral Order, *J. Phys. Chem. Lett.*, 2018, **9**, 1012-1017.
6. X. E. Wu, W. J. Lu, L. M. Streacker, H. S. Ashbaugh and D. Ben-Amotz, Methane Hydration-Shell Structure and Fragility, *Angew. Chem.-Int. Edit.*, 2018, **57**, 15133-15137.
7. F. Bohm, G. Schwaab and M. Havenith, Mapping Hydration Water around Alcohol Chains by THz Calorimetry, *Angew. Chem.-Int. Edit.*, 2017, **56**, 9981-9985.
8. B. Hess, C. Kutzner, D. van der Spoel and E. Lindahl, GROMACS 4: Algorithms for highly efficient, load-balanced, and scalable molecular simulation, *J. Chem. Theory Comput.*, 2008, **4**, 435-447.
9. B. Chen, J. J. Potoff and J. I. Siepmann, Monte Carlo calculations for alcohols and their mixtures with alkanes. Transferable potentials for phase equilibria. 5. United-atom description of primary, secondary, and tertiary alcohols, *J. Phys. Chem. B*, 2001, **105**, 3093-3104.
10. J. L. F. Abascal and C. Vega, A general purpose model for the condensed phases of water: TIP4P/2005, *J. Chem. Phys.*, 2005, **123**.